Neuron, Volume *109*

Supplemental information

Coordination of escape and spatial navigation circuits orchestrates versatile flight from threats

Weisheng Wang, Peter J. Schuette, Jun Nagai, Brooke Christine Tobias, Fernando Midea Cuccovia V. Reis, Shiyu Ji, Miguel A.X. de Lima, Mimi Q. La-Vu, Sandra Maesta-Pereira, Meghmik Chakerian, Saskia J. Leonard, Lilly Lin, Amie L. Severino, Catherine M. Cahill, Newton S. Canteras, Baljit S. Khakh, Jonathan C. Kao, and Avishek Adhikari

SUPPLEMENTAL FIGURES

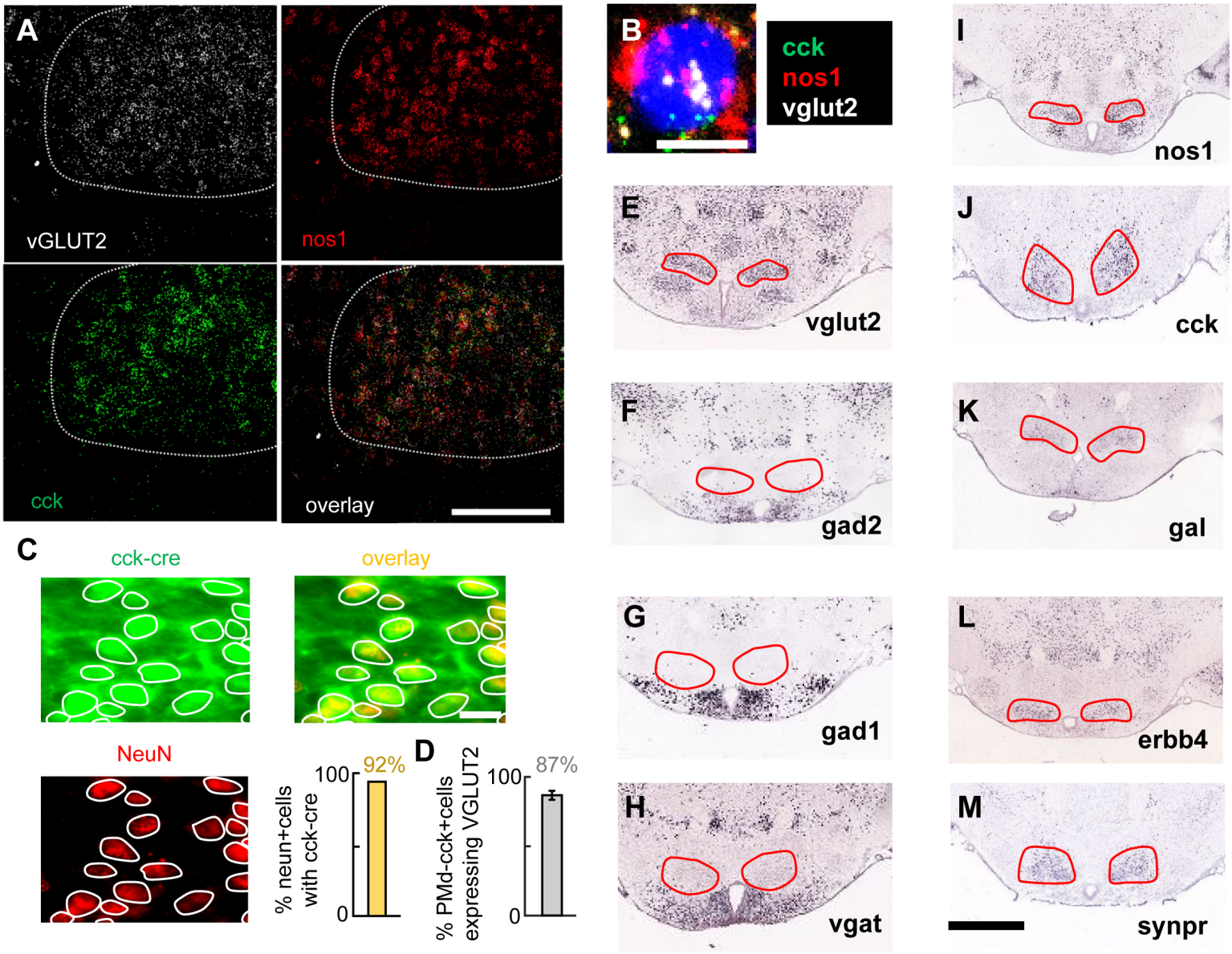

Figure S1. PMd cells express VGLUT2 and cck, Related to Figure 1.

(A) *In situ* hybridizations in the PMd (PMd boundaries are shown in white dashed line) show high expression of vglut2, nos1 and cck. (scalebar: 150 μm)

(B) Example neuron showing co-localization of all 3 markers. (scale bar: 10 μm)

(C) Cck-cre mice were injected with AAV9-EF1a-DIO-YFP in the PMd. The images show the high degree of co-localization between YFP expression and the pan-neuronal marker NeuN, indicating that the majority of PMd neurons express cck. (scalebar: 20 μm)

(D) Bar depicts the percent of PMd-cck+ cells that express VGLUT2. (Mean ± SEM)

(E-H) Images from the Allen Brain Institute gene expression database showing that glutamatergic, but not GABAergic markers are expressed in the PMd.

(I-M). Genes highly expressed in the PMd include nos1, cck, gal (galanin), erbb4 and synpr.

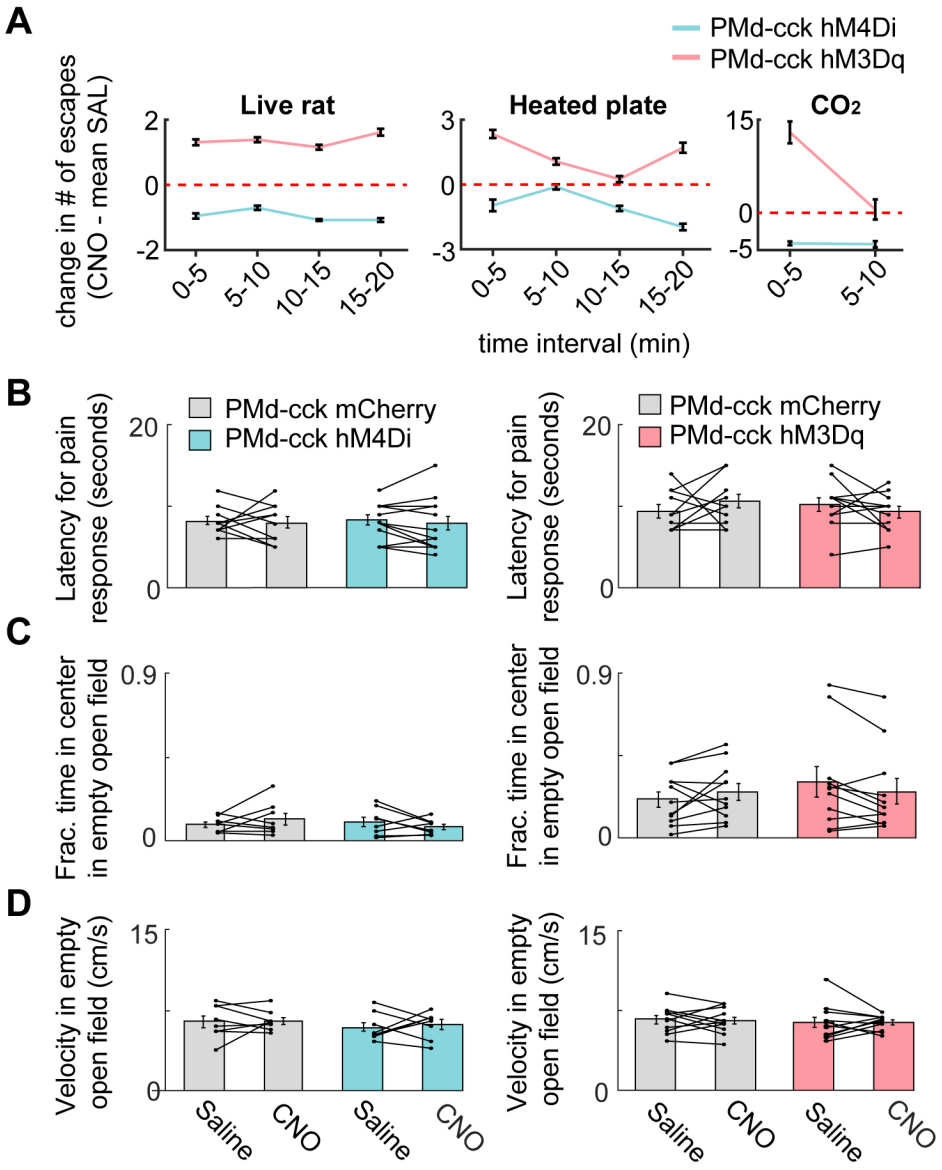

Figure S2. Chemogenetic manipulations in PMd-cck cells altered escape but not pain sensitivity, anxiety or velocity, Related to Figure 1.

(A) Lines show the change in the number of escapes (CNO - mean saline; +/- 1 s.e.m.) for the rat (left), heated plate (middle) and CO_2 (right) assays at consecutive time intervals. (live rat (hM4Di): mCherry *n*=14, hM4Di *n*=16; live rat (hM3Dq): mCherry *n*=12, hM3Dq *n*=13; heated floor (hM4Di): mCherry *n*=7, hM4Di *n*=7; heated floor (hM3Dq): mCherry *n*=11, hM3Dq *n*=11; CO_2 (hM4Di): mCherry *n*=7, hM4Di *n*=11; CO_2 (hM3Dq): mCherry *n*=7, hM3Dq *n*=8).

(B) Mice were placed on a floor heated at 55^{O}C. The latency to show pain-related responses (jumping or paw-licking) was recorded, and then mice were moved back into their home cage. All mice displayed a pain-related response within 30 seconds. Mice-expressing hM4Di or hM3Dq in PMd-cck cells did not show altered pain responses in the hot plate test during treatment with CNO compared to saline treatment (mCherry/hM4Di *n*=10, *n*=13; mCherry/hM4Dq *n*=11, *n*=11).

(C,D) Mice-expressing hM4Di or hM3Dq in PMd-cck cells do not show changes in anxiety-related time spent in center (C) or velocity (D) during CNO compared to saline treatment. (mCherry/hM4Di *n*=8, *n*=8; mCherry/hM4Dq *n*=11, *n*=11) Mean ± SEM.

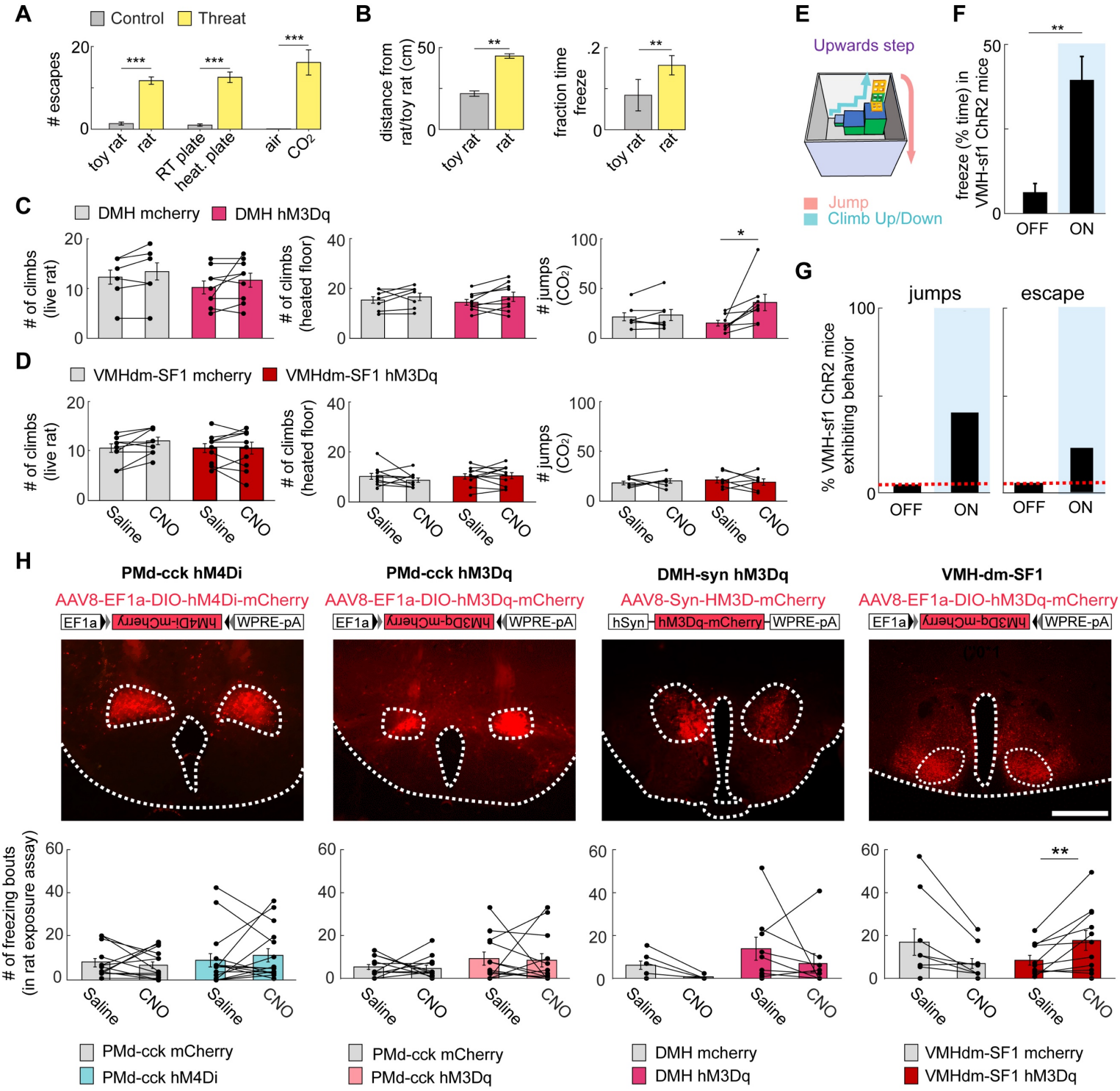

Figure S3. Chemogenetic excitation of dorsomedial and ventromedial hypothalamic nuclei do not elicit context-specific escape, Related to Figure 1.

(A) Bars depict the number of escapes in each threat and related control assay for all mCherry control mice in saline sessions. (toy rat n=18; rat n=26; room temperature plate n=17; heated plate n=18; air n=18; CO_2 n=14) (Wilcoxon signed-rank test, ***p<0.001)

(B) Bars depict the mean distance (left) of mice from the rat/toy rat and the fraction of time mice exhibited freezing behavior (right) in the rat/toy rat assays. (*n* same as in (A)) (Wilcoxon signed-rank test, **p<0.01, ***p<0.001)

(C) Mice were injected with AAV9-syn-mCherry or AAV9-syn-hM3Dq-mCherry in the dorsomedial hypothalamus (DMH). DMH-syn excitation only increased panic-related jumping to CO_2 (Two-way repeated measures ANOVA followed by

Wilcoxon test, *p = 0.008), but not the more complex climbing escapes in the rat or heated floor assay. (live rat: mCherry *n*=7, hM3Dq *n*=9; heated floor: mCherry *n*=7, hM3Dq *n*=9; CO_2: mCherry *n*=7, hM3Dq *n*=8).
(D**)** Same as (C), but for but for mice injected with AAV8-EF1a-DIO-mCherry or AAV8-EF1a-DIO-hM3Dq-mCherry in the dorsomedial portion of the ventromedial hypothalamus (VMHdm) of SF1-cre mice. Excitation of VMHdm-SF1 cells did not increase escape in any assay tested. (live rat: n=10 mCherry, 11 hM3Dq; heated plate: n=10 mCherry, 11 hM3Dq; CO_2: n=7 mCherry, 7 hM3Dq)
(E) VMH-sf1 mice were optogenetically stimulated (3 mins OFF/3 mins ON/3 mins OFF) in the upwards step assay.
(F) Bars show the % time freezing (n=5).
(G) Bars depict (left) the number of mice to exhibit jumps and (right) escape the enclosure during light ON and light OFF (n=5).
(H) Upper row: Images showing expression of excitatory and inhibitory chemogenetic modulators in PMd-cck cells, dorsomedial hypothalamus (DMH)-synapsin cells and VMHdm-SF1 cells. (scale bar: 500 μm) Lower row: Freezing bouts are increased in VMHdm-SF1 mice treated with CNO during exposure to the rat assay. (two-way repeated measures ANOVA followed by post hoc Wilcoxon test, **p < 0.01). n = (14 PMd-cck mCherry, 16 PMd-cck hM4Di), n = (12 PMd-cck mCherry, 13 PMd-cck hM3Dq), n = (6 DMH-syn mCherry, 9 DMH-syn hM3Dq), n = (9 VMHdm-SF1 mCherry,11 VMHdm-SF1 hM3Dq). Mean ± SEM.

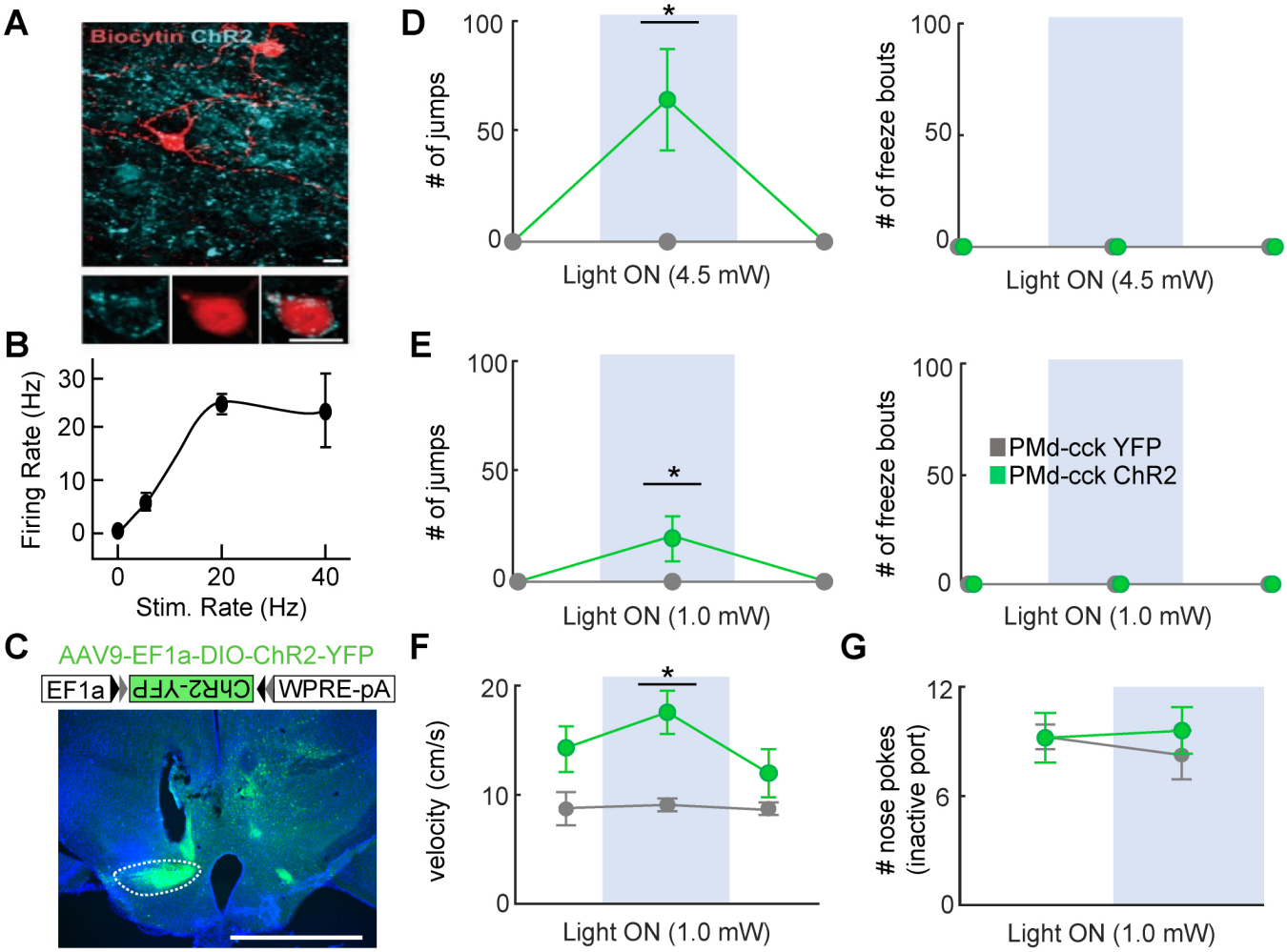

Figure S4. PMd-cck optogenetic activation selectively causes escape but not other defensive behaviors, Related to Figure 2.

(A) *Ex vivo* slices were prepared from cck-cre mice injected with AAV9-EF1a-DIO-ChR2-YFP in the PMd. Recorded PMd-cck neurons expressing ChR2 were filled with biocytin at the end of the experiment. Image showing biocytin-filled PMd-cck neuron (red) and ChR2-YFP (blue). (both scale bars = 10 μm)

(B) Plot showing firing rate in ChR2-expressing PMd-cck cells stimulated with blue light trains of 0, 5, 20 and 40 Hz.

(C) Image showing ChR2-GFP expression in PMd-cck cells along with fiber optic cannula track above the PMd. PMd outline is shown in white. (scale bar:1 mm)

(D,E) Activation of PMd-cck cells optogenetically increased jumps, but not freezing, both at 4.5 mW (D) and 1 mW (E) stimulation intensities.

(F) PMd-cck activation also increased velocity.

(D-F) (For each behavioral measure, YFP *n*=4, ChR2 *n*=4, Wilcoxon rank-sum test, light-on epoch, *p<0.05).

(G) PMd-cck activation caused no change in the number of nose pokes when poke did not stop stimulation. (YFP n=4, ChR2 n=5).

(B,D-G) Mean ± SEM.

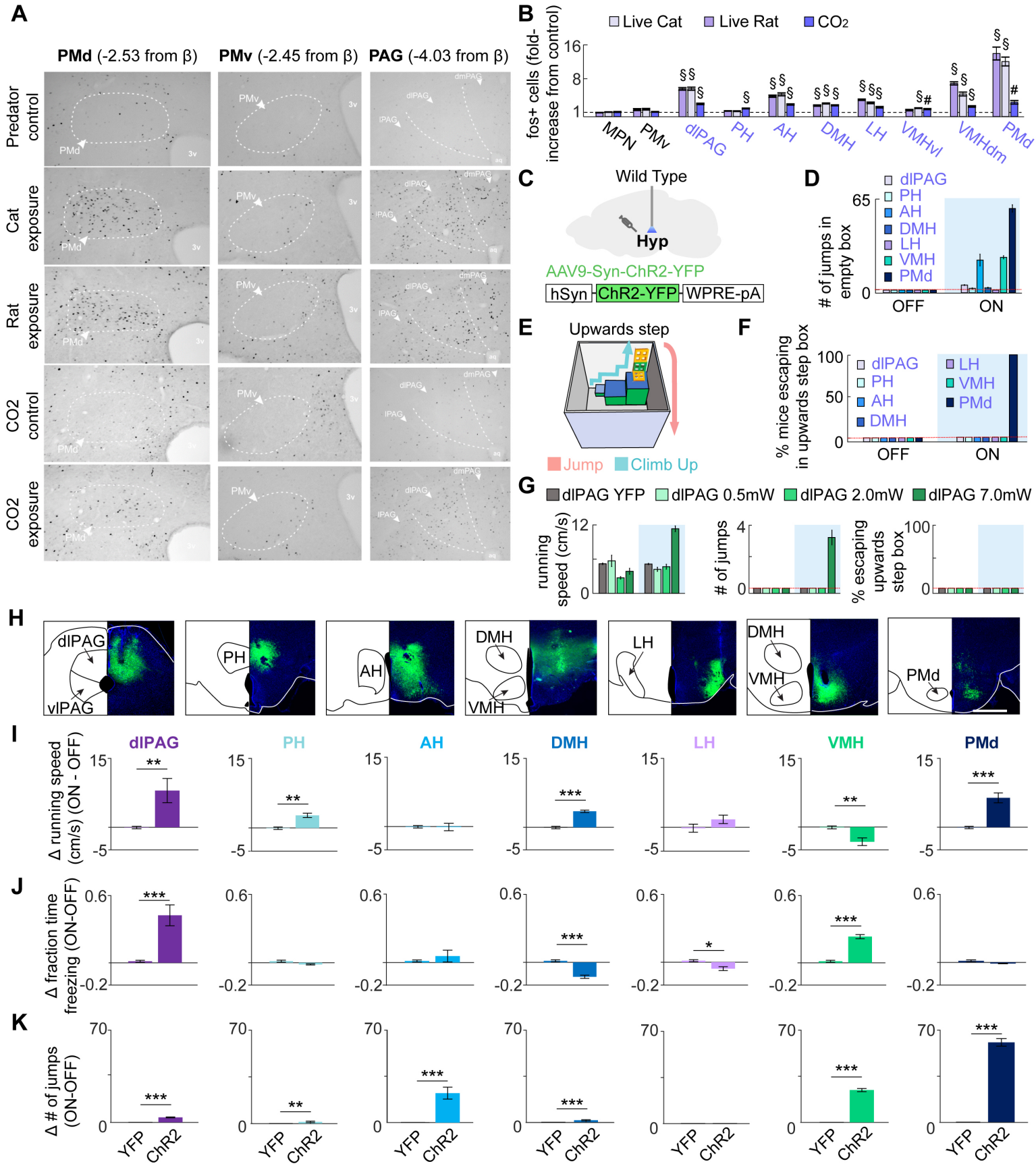

Figure S5. Dorsal premammillary nucleus (PMd) optogenetic stimulation induces versatile context specific escape from novel environments and defensive behaviors for regions with threat-induced increases in fos expression, Related to Figure 2.

(A) Images show PMd, PMv and dlPAG sections stained with antibody against fos in mice exposed to cat, rat, CO_2 and control conditions. Threat exposure increases fos in PMd and dlPAG. Abbreviations: PMd (dorsal premammillary nucleus), l, dl and dm PAG (lateral, dorsolateral and dorsomedial periaqueductal gray respectively), PMv (ventral premammillary nucleus).
(B) Expression of fos in select hypothalamic and brainstem nuclei following exposure to live predators or 15% CO_2. Significantly activated regions are shown in purple. Abbreviations: MPN (median preoptic nucleus), PMv (ventral premammillary nucleus), dlPAG (dorsolateral periaqueductal gray), PH, AH, DMH and LH (posterior, anterior, dorsomedial and lateral hypothalamus, respectively), VMHvl and VMHdm (ventrolateral and dorsomedial ventromedial hypothalamus), PMd (dorsal premammillary nucleus). The PMd showed the highest fos induction during threat exposure compared to other regions (each region, n=5, two-way independent ANOVA (rat/cat), two-tailed t-test (CO_2), § $p < 0.005$, # $p < 0.01$).
(C) Mice were injected with AAV9-syn-ChR2-YFP and had fiberoptic cannulae implanted in regions that showed increased fos expression in (B).
(D) These regions (D) were optogenetically activated with blue light in wild type mice in an empty open field box (473 nm, 20 Hz, 3 minutes OFF, 3 minutes ON). The number of jumps displayed is plotted. (D,F) Dashed red line indicates zero.
(E) Side view of the complex route to escape from a novel environment using upwards climbing. Mice had no exposure to this context prior to the test.
(F) Regions in (D) were optogenetically activated in the environment shown in (E) (473 nm, 20 Hz, alternating OFF-ON epochs, for a total of 5 minutes. Each OFF and each ON epoch lasted 30 seconds). Only optogenetic stimulation of the PMd caused escape from this environment before the end of the five-minute assay. (n=5 ChR2 for each brain region).
(G) Mice were injected with AAV9-syn-ChR2-YFP and fiberoptic cannulae were implanted over the dlPAG (n=5). Bars depict running speed (left), the number of jumps (middle) and the percent mice to escape the upwards step box for YFP controls and ChR2 mice at three levels of blue light intensity (0.5, 2.0 and 7.0 mW) for light OFF and light ON epochs.
(H) Mice were injected with AAV9-syn-YFP in various hypothalamic nuclei and the dorsal periaqueductal gray. Images show expression of YFP (green) in representative coronal sections. (scale bar: 1 mm) Abbreviations: (dorsal periaqueductal gray), PH, AH, DMH and LH (posterior, anterior, dorsomedial and lateral hypothalamus, respectively), VMHvl and VMHdm (ventrolateral and dorsomedial ventromedial hypothalamus), PMd (dorsal premammillary nucleus).
(I-K) All regions showing significant increases in fos expression following exposure to threats (B) were optogenetically activated in wild type mice in an empty open field box. Mice were injected with AAV9-syn-ChR2-YFP in the target structure and light was delivered in 20 Hz 5-ms pulses. Bar plots showing increases in running speed (I), freezing (J) and escape jumps (K) following optogenetic stimulation. YFP controls for activated nuclei did not differ in any of the measured behaviors and were thus pooled together (Pooled YFP n=25, dlPAG n=5, PH n=5, AH n=6, DMH n=5, LH n=5, VMH n=5, PMd n=5) The ON-OFF difference was compared between YFP and ChR2 groups by two sample t-test; *$p < 0.05$, **$p < 0.01$, ***$p < 0.001$).
(B,D,G,I-K) Mean ± SEM. See full statistical details for all Figures in Table S1.

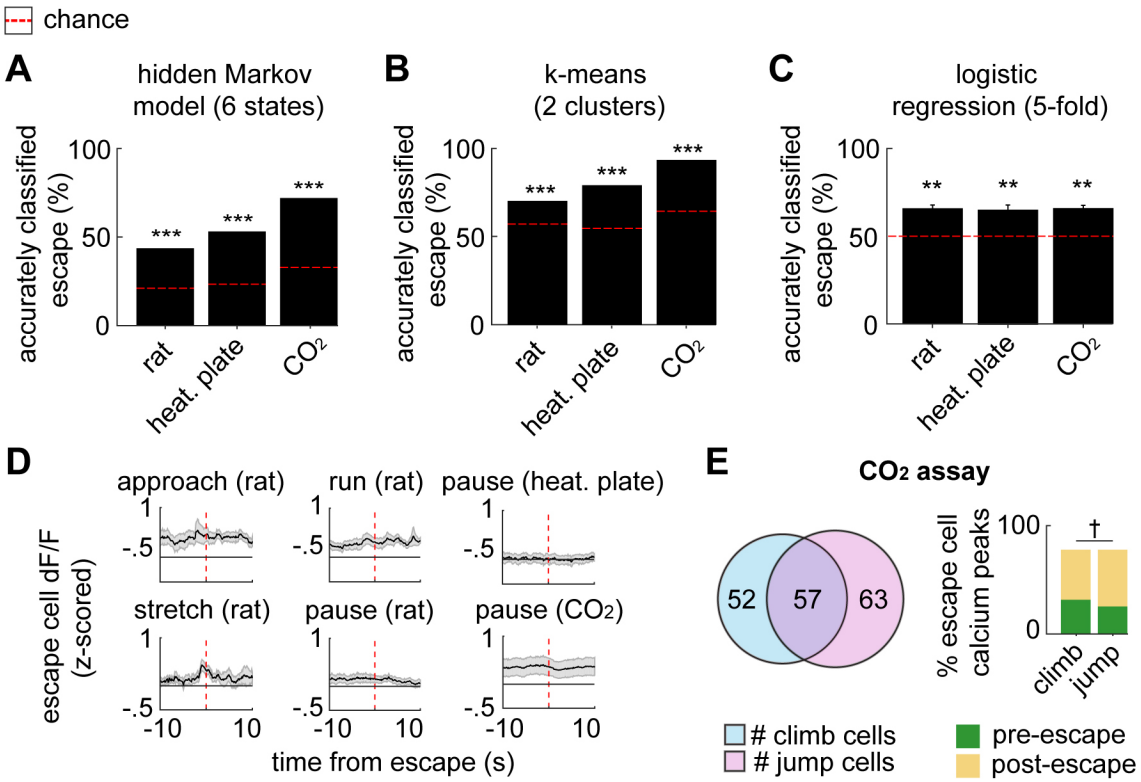

Figure S6. Supervised and unsupervised analyses significantly predict escape from neural data, Related to Figure 3.

(A) The states extracted by hidden Markov model (6 states) predicted escape at a level significantly greater than chance (red lines) for each threat assay. (p<.001)

(B) Similar to (A), using *k*-means, an alternative unsupervised technique, two clusters could predict escape at a level significantly greater than chance (red lines) for each threat assay.

(C) Using 5-fold logistic regression, escape could be predicted for each assay at a level significantly greater than chance (red line). (rat n=10, heated plate n=9, CO_2 n=8) Mean ± SEM.

(D) Lines show the mean z-scored signal (+/- 1 SEM) for escape-categorized cells, aligned to behavioral onsets occurring within -10 to 10 seconds of an escape (rat: *n*=10; heated plate: *n*=9; CO_2 : *n*=12).

(E) (left) Venn diagram depicts the overlap in climb- and jump-classified cells in the CO_2 assay (climb cell *n*=109, jump cell *n*=120, session *n*=9). (right) Bars depict the percentage of exclusive climb- and jump-categorized cell calcium peaks that occurred pre- (green) or post- (yellow) escape. (pre-escape *n*=97, post-escape *n*=144; jump: pre-escape *n*=145, post-escape *n*=297; Fisher's exact test, † p=0.055)

(A-C) ** p<.01, ***p<.001.

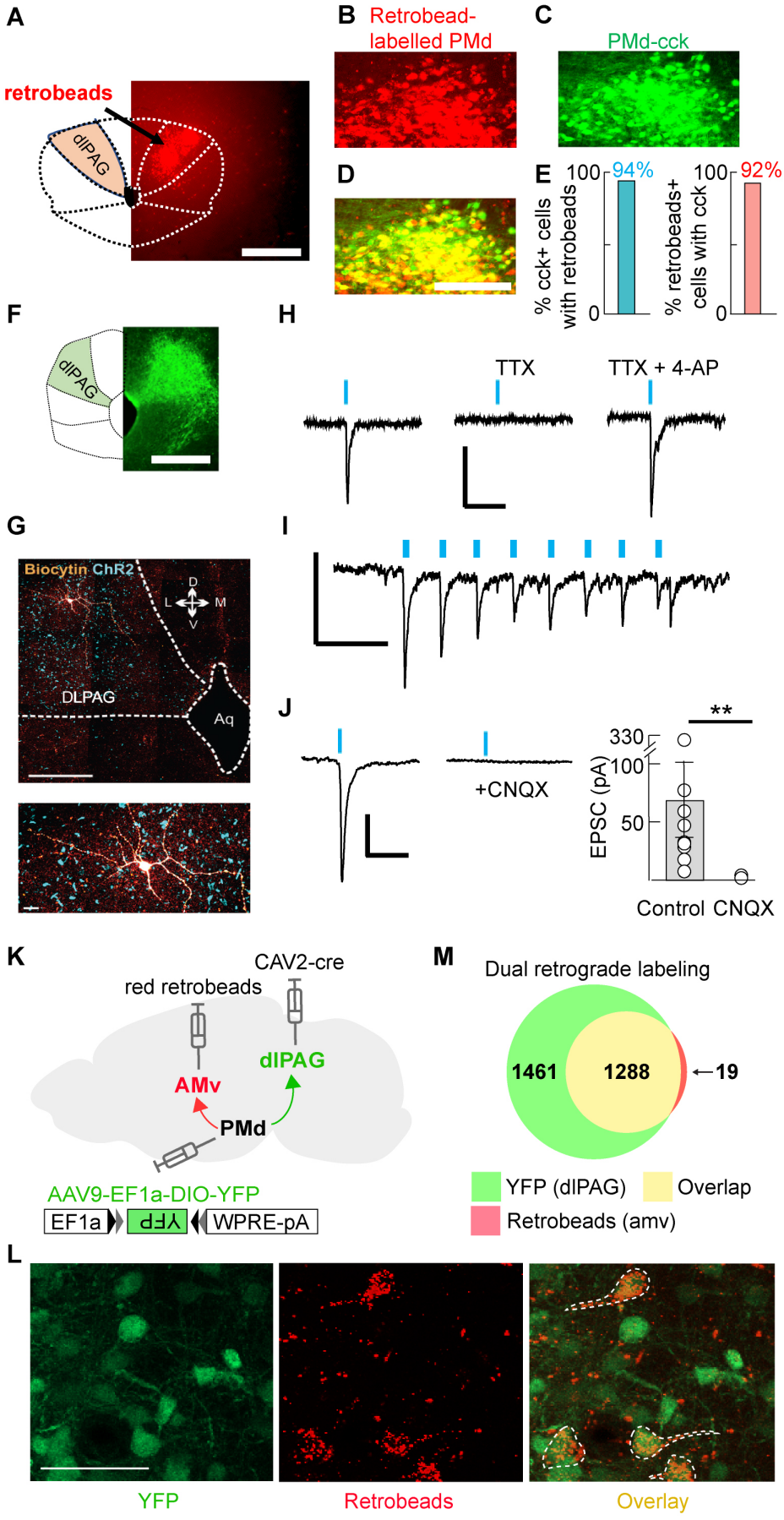

Figure S7. Anatomical and functional characterization of the PMd-cck to dlPAG projection and characterization of PMd projections to amv and dlPAG, Related to Figure 4.

(A) Retrobeads were injected in the dlPAG in cck-cre mice expressing cre-dependent YFP in the PMd. (scale bar: 500 μm)
(B) Presynaptic dlPAG-projecting PMd cells with retrobeads.
(C) YFP expression in PMd-cck cells.
(D) Overlay. (scale bar: 250 μm)
(E) Quantification of overlap between dlPAG-projecting and cck-cre expressing cells.
(F) GFP-expressing PMd-cck axon terminals in the dlPAG. (scale bar: 500 μm)
(G) (top) Photograph showing biocytin filled dlPAG neuron (orange) and ChR2-expressing PMd-cck (blue). (scale bar: 200 μm) (bottom) Higher magnification image of the dlPAG cell from the top panel.
(H) (left) dlPAG cell shown in (G) showed excitatory response following blue light delivery to excite ChR2-expressing PMd-cck axon terminals in an *ex vivo* slice preparation. (middle) The response disappeared following application of tetrodotoxin (TTX, 0.3 μM). (right) The response was rescued following the application of the potassium channel blocker 4-aminopiridine (4-AP, 0.5 mM). (scale bar: 50 ms, 20 pA). Aq: aqueduct
(I) Overlaid traces of dlPAG cell showing responses to 20 Hz 5ms train stimulation of ChR2-expressing PMd-cck axon terminals. (scale bar: 100 ms, 20 pA)
(J) dlPAG responses to stimulation of PMd-cck terminals were abolished in the presence of the glutamatergic AMPA/kainate receptor blocker cyanquixaline (CNQX, 20 μM). (scale bar: 50 ms, 20 pA) (Control n=9, CNQX n=9; Wilcoxon rank-sum test, **p = 0.009; Mean ± SEM).
(K) Scheme showing approach to label PMd cells projecting to amv and dlPAG. Red retrobeads were injected in the amv, retrograde CAV2-cre was injected in the dlPAG and AAV9-EF1a-DIO-YFP was injected in the PMd.
(L) Representative images showing YFP-expressing and retrobead containing PMd cells, which respectively project to the dlPAG and amv. Double-labelled cells projecting to both regions are shown with a white dashed outline. (scale bar: 50 μm)
(M) Venn diagram showing the overlap of YFP and retrobead-labelled cells in the PMd. (n=4 mice; 2768 cells)

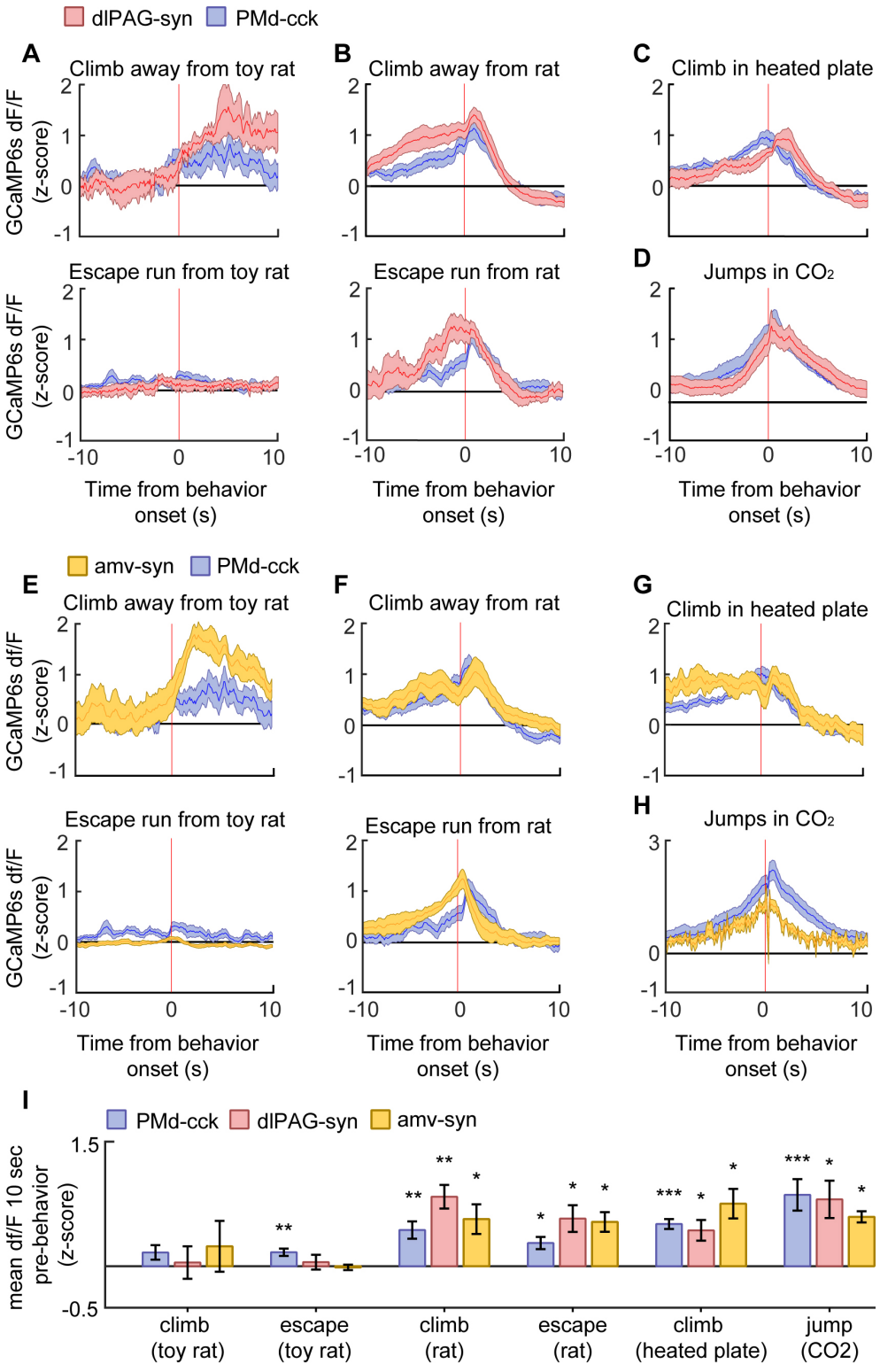

Figure S8. Behavior-aligned photometry signals from PMd-cck/dlPAG-syn and PMd-cck/amv-syn during escape behaviors, Related to Figure 4.

(A-D) Dual-site fiber photometry recordings were performed in cck-cre mice injected with AAV9-Ef1a-DIO-GCaMP6s-YFP and AAV9-syn-GCaMP6s-YFP respectively in the PMd and the dlPAG.

(A) Average photometry signals centered around climb and escape run in toy rat assay (*n*=9).

(B) Same as (A), but for rat exposure (*n*=9).

(C) Average PMd-cck and dlPAG photometry signals centered around climbs in the heated floor assay. (*n*=8)

(D) Same as (A) but for jumps during CO_2 exposure. (*n*=9)

(E-H), Same as (A-D), but for dual-site fiber photometry recordings performed in cck-cre mice injected with AAV9-Ef1a-DIO-GCaMP6s-YFP and AAV9-syn-GCaMP6s-YFP respectively in the PMd and the amv. (*n*=7 for rat and CO_2 assays and controls; *n*=6 for heated plate assay)
(I) In all threat assays, PMd-cck, dlPAG and amv neural activity increased prior to escape. (Wilcoxon signed-rank test, * p<.05, ** p<.01, ***p<.001)
(A-I) Mean ± SEM.